

# Modelling thermal parasitic load lines for an optical refrigerator

K W Martin<sup>1,3</sup>, J Shomacker<sup>2</sup>, T Fraser<sup>3</sup>, and C Dodson<sup>3</sup>

<sup>1</sup>Applied Technology Associates 1300 Britt St. SE Albuquerque, NM 87123-3353

<sup>2</sup>Rensselaer Polytechnic Institute 110 8<sup>th</sup> St. Troy, NY 12180

<sup>3</sup>Spacecraft Component Thermal Research Group at Air Force Research Labs Kirtland AFB, NM 87117-5776

Email: Kyle.martin.19.ctr@us.af.mil

**Abstract.** Optical refrigeration is currently the only completely solid state cooling method capable of reaching cryogenic temperatures from room temperature. Optical cooling utilizing Yb:YLF as the refrigerant crystal has resulted in temperatures lower than 123K measured via a fluorescence thermometry technique. However, to be useful as a refrigerator this cooling crystal must be attached to a sensor or other payload. The phenomenology behind laser cooling, known as anti-Stokes fluorescence, has a relatively low efficiency which makes the system level optimization and limitation of parasitic losses imperative. We propose and model a variety of potential designs for a final optical refrigerator, enclosure and thermal link; calculate conductive and radiative losses, and estimate direct fluorescence reabsorption. We generate parasitic load-lines; these curves define temperature-dependent minimum heat lift thresholds that must be achieved to generate cooling for detectors.

## 1. Introduction

Optical refrigeration (OR) presents a unique approach to satisfy cryogenic cooling needs. OR of rare earth doped insulator crystals, specifically ytterbium doped yttrium lithium fluoride (Yb:YLF), have shown the most promise for generating necessary cooling for infrared detectors, cooling below the NIST cryogenic standard of 123 K [1]. Insulator crystal OR utilizes an anti-Stokes phenomena [2] to generate cooling, using a photon to extract the crystal phonon energy and convert it to a higher energy photon. Doping the YLF crystal with a Yb<sup>3+</sup> ion splits the degenerate electronic states of the Yb<sup>3+</sup> ion, called crystal-field splitting, see figure 1 [3,4]. A laser tuned to frequency,

$$\nu = \frac{E5 - E4}{h}, \quad (1)$$

is incident on the cooling crystal, promoting an electron from the E4 to the E5 energy level. After the electron is promoted to the excited manifold the atom thermalizes, absorbing phonons from the crystal. The atom will then spontaneously emit a photon at frequency  $\nu_f > \nu$ . Through this process Melgaard et al. were able to achieve a no load temperature of 93 K from a reject temperature of 271 K [5].



$$\eta_{cool} = \eta_{ext} \left[ \frac{1}{1 + \alpha_b / \alpha(\lambda, T)} \right] \frac{\lambda}{\lambda_f(T)} - 1, \quad (2)$$

The anti-Stokes phenomenon is rather inefficient, requiring multiple passes through the cooling crystal in a non-resonant cavity to achieve this temperature. This cooling efficiency is given by equation 2 [1,3,4], where,  $\alpha_b$  is the background absorption,  $\alpha(\lambda, T)$  is the temperature and wavelength dependent resonant absorption,  $\lambda_f(T)$  is the temperature dependent fluoresced frequency,  $\lambda$  is the laser wavelength, and  $\eta_{ext}$  is the external quantum efficiency. External quantum efficiency and background absorption drive the cooling efficiency of the Yb:YLF crystal. An external quantum efficiency of 99.5% and  $\alpha_b = 2.0 \times 10^{-4} \text{cm}^{-1}$  were required for the record breaking temperature achieved in [5]. The minimum achievable temperature (MAT) map for this crystal is shown in figure 2.

Although great progress has been made in low temperatures achieved by OR, all temperature measurements were made via a differential luminescence thermometry (DLT) technique and no device (thermistor, IR sensor, etc.) has been cooled to date. DLT measures the temperature-dependent fluorescence emanating from the crystal and utilizes a calibration curve to determine the crystal temperature [6]. Our desire is to develop an entirely solid-state cryogenic cooler that minimizes parasitic heating while providing useful cooling to a payload or sensor. Thermal modeling provides a first step in the design process.

## 2. Thermal losses for an optical refrigerator

For our simulations we utilize a CAD based thermal modelling software, Thermal Desktop<sup>TM</sup>. This program allows the user to develop radiative, conductive and convective heat transfer models for solids and surfaces.

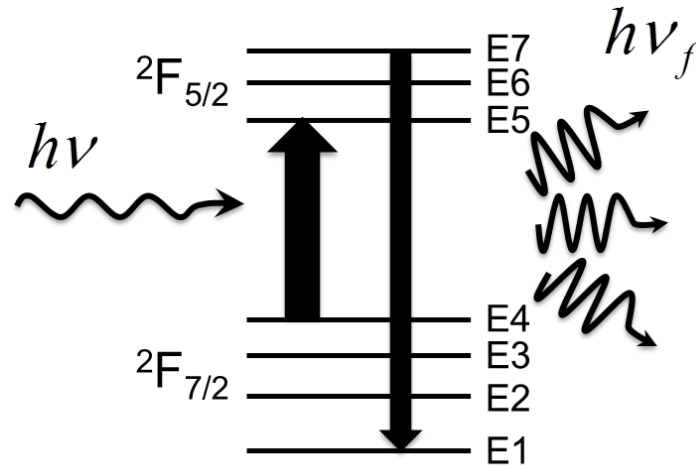


**FIGURE 1.** Shows the cooling cycle of insulator crystal optical refrigeration. Absorption of laser light promotes an electron from the ground state to the excited state manifold. The atom thermalizes, spontaneously emits at a frequency  $\nu_f > \nu$ . The atom thermalizes to the E4 energy level and repeats.

Designing an efficient all solid-state optical refrigerator requires a minimization and understanding of the parasitic thermal losses of such a device. There are other thermal loss mechanisms associated with designing an optical refrigerator, but we only focus on radiative, conductive, and an estimated direct fluorescence absorption loss. We mention the other thermal loss mechanisms for completeness, but they are ignored in our simulations.

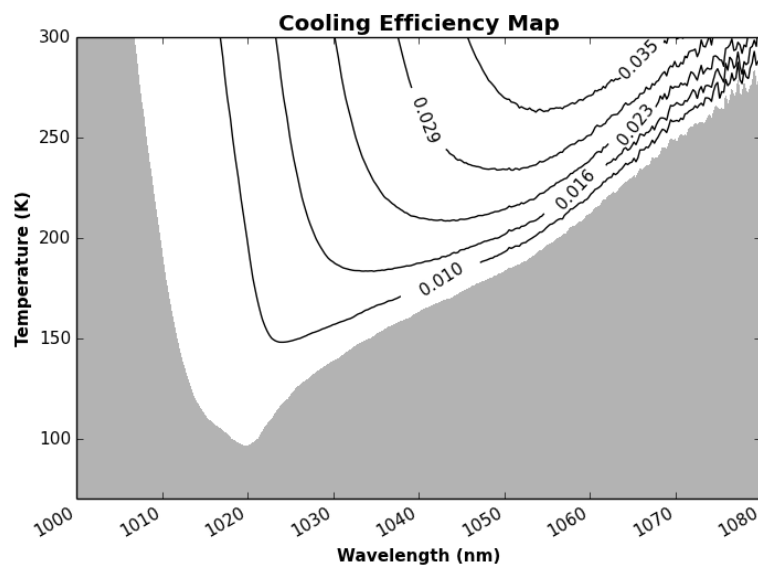


**FIGURE 2.** The minimum achievable temperature (MAT) map for a 10% Yb:YLF crystal with an external quantum efficiency of 99.5% and  $\alpha_b = 2.0 \times 10^{-4} \text{ cm}^{-1}$ . The minimum predicted temperature of this crystal is 93 K. The shaded area of the MAT is the heating region while the white contour plot details cooling efficiency, cooling power over absorbed power.

For our thermal model we ignore convection, indirectly reabsorbed fluorescence, Kapitza resistance, and as well as optical losses. We can ignore convective heat transfer because the proposed design will be in a hard vacuum environment ( $< 10^{-6}$  torr). There is also a potential for fluoresced photons to be reabsorbed as heat. To avoid indirect fluorescence exposure, reabsorption by the cooling crystal, we plan to enclose the crystal in a light tight box, with high absorption in the fluoresced wavelengths. To reduce direct fluorescence exposure, i.e. absorption by the payload mount causing parasitic heating, we plan to build a tortuous, optically clear path from the crystal to the payload mount using sapphire. This will allow most of the fluoresced photons to escape [3,7]. Indirectly reabsorbed fluorescence is the largest loss mechanism that we ignore. Thermal Desktop has no way to simulate either fluorescence mechanism, but we estimate direct fluorescence losses.

### 2.1 Conductive Losses

The thermal link and YLF cooling crystal must be suspended and aligned in the beam path. One end of the suspension will be thermal strapped to the reject temperature and one end will be anchored to the cold tip. This suspension system will introduce a parasitic thermal path that must be minimized.

Adiabatic demagnetization routines commonly use a Kevlar<sup>T.M.</sup> cat's cradle suspension system to provide rigid support while maintaining low conductive losses [9]. This takes advantage of Kevlar's low thermal conductivity properties and high strength to further reduce the thermal conductance by reducing the contact area. Unfortunately, Kevlar has a negative coefficient of thermal expansion and a suspension system that maintains crystal/laser alignment would most likely require a more complicated design with a tensioner [10].

Recent advances in aerogel have produced a rigid material with very low thermal conductivities which can be machined, but would require a more substantial mounting contact area [11]. Using aerogel would alleviate the manufacturing/design difficulty and the potential misalignment from cooling a Kevlar suspension system, aerogel could also be more robust to vibration and shock. The

consequence of manufacturing a support from aerogel would be an added conductive parasitic loss. We examine a non-optimal aerogel support system design here to determine its potential usefulness in future optical refrigeration designs.

## 2.2 Radiative losses

The entire cooler must be enclosed to prevent the fluorescence from irradiating the payload. The enclosure will present a surface for radiative heat transfer. Both surfaces will be gray bodies and will follow the gray body enclosure heat transfer equation [12,13], equation 3 shows this law for two surfaces.

$$\dot{Q}_{2 \rightarrow 1} = \frac{\sigma(T_2^4 - T_1^4)}{\frac{1 - \epsilon_1}{A_1 \epsilon_1} + \frac{1}{A_2 F_{2 \rightarrow 1}} + \frac{1 - \epsilon_2}{A_2 \epsilon_2}} \quad (3)$$

We plan on coating the interior of the enclosure with an Acktar nano-black<sup>T.M.</sup> solar selective coating. This material has a very low emissivity in the long wave infrared, to reduce radiative heat transfer, but has large absorbance in the fluoresced wavelengths, to reduce indirect and direct fluoresced light heat transfer [14].

## 3. Thermal Link Model and Design

The optical refrigerator proposed is modelled using Thermal Desktop [15]. All material interfaces are modelled to be perfect conductors, ignoring the Kapitza resistance, this is highly idealized and would have to be measured in the final device. A sapphire arm is to be bonded to the YLF crystal allowing an optically clear path for fluoresced photons to escape. We examined two designs, a simple “L” geometry shown in Figure 3a, and a more complex “Tetris” geometry, shown in Figure 3b. Both geometries were proposed by Richard Epstein et al. [7].

Zemax modelling predicts that 0.16 % of the light entering the thermal link for the “L” link and 0.025% for the “Tetris” link will be absorbed by the titanium layer causing heating [3,7]. We assume that if the crystal absorbs 24 W, 4 W enters the thermal link, based on geometry. Heater nodes are defined at the titanium/sapphire interface to simulate the absorbed fluorescence on this surface, 6.4 mW for the “L” link and 1 mW for the “Tetris” link. The “L” and “Tetris” geometries highlight a trade-off between indirectly absorbed fluorescence and radiation losses. The “Tetris” link rejects more fluorescence, but has a larger exposed surface area for radiative heat transfer.

5 nm of titanium followed by 50 nm of gold are proposed to transition the sapphire link to copper, on which the payload will be mounted, see Figure 3. The 50 nm gold layer is there to minimize the thermal contact resistance from titanium to copper; the Kapitza resistances from YLF to sapphire and sapphire to titanium are unknown. For modelling ease the titanium and gold features have been enlarged to 0.1 mm and 0.5 mm respectively.

Ideally, an enclosure with an interior coating of Acktar Nano-Black solar selective coating surrounds the proposed cold head. The same series of enclosures are utilized for the “Tetris” and “L” geometries. The enclosures utilized were: an Acktar Nano-Black coated cube side length 40 mm and a tight enclosure whose walls were 1 mm from the crystal/link. The cold head temperature was varied from 100 K to 250 K while holding the reject temperature at 300 K. We also varied the reject temperature from 270 K to 300 K while holding the cold head temperature at 100 K. Finally, for the support design, we utilized both Kevlar and aerogel. The Kevlar support system is simplified to be 8 Kevlar threads extending 1 cm from the copper link and the final node held at reject temperature. The aerogel design encases the entire copper link and also extends 1 cm to reject temperature. The aerogel

design is not optimized to reduce parasitic heat load, but increasing the length and decreasing the contact area of the support will reduce conductive parasitic losses. It is still unknown how small an aerogel support can be made and still maintain a rigid structural system; an initial iterative design/build process will help answer this question. Although not minimized, the aerogel support simulation was performed to ensure that aerogel losses were manageable.

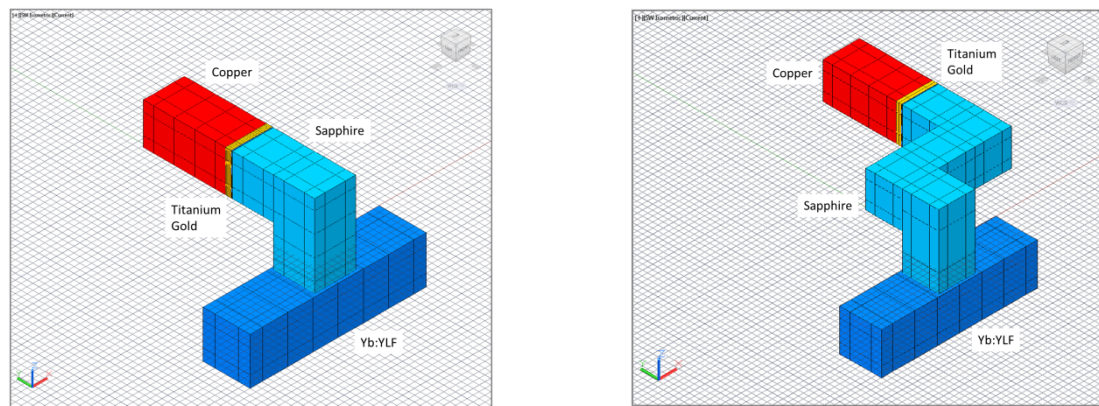


**FIGURE 3.** Shown above are the proposed optical link geometries. The link provides a thermal path to a conductive metal payload mounting surface while maintaining an escape path for fluoresced photons. The “Tetris” link (shown on the left) is expected to allow more fluorescence to escape than the “L” link (shown on the right).

#### 4. Results

The “Tetris” link was proposed to reduce the absorbed fluorescence on the titanium surface; this reduction of parasitic loss is predicted to be 5.4 mW. However, by increasing the crystal/link surface area we also increase the radiative heat transfer. Increasing the tortuous path for our simulated coolers had an overall negative effect, increasing the total parasitic heat transfer [19].

Simulation	Support	Link Geometry	Enclosure Geometry
1	Aerogel	L-link	Tight
2	Kevlar	L-link	Tight
3	Aerogel	Tetris-link	Tight
4	Kevlar	Tetris-link	Tight
5	Kevlar	Tetris-link	Acktar Cube
6	Aerogel	Tetris-link	Acktar Cube
7	Aerogel	L-link	Acktar Cube
8	Kevlar	L-link	Acktar Cube

**TABLE 1.** Shown above are the geometries for each simulation. The results from these simulations can be found in figure 4.

The geometry that best reduced thermal parasitics for all reject temperatures and cold tip temperatures was the L-link supported by Kevlar thread in a tight enclosure, results detailed in figure 4 and table 1. The aerogel support was proposed to ease manufacturability as well as eliminate optical alignment issues, neither of which conditions was examined here. The aerogel support design was also not optimized, needing more information on the minimum surface contact area and maximum structural length that could provide a rigid mounting system. The Kevlar outperformed the simulated aerogel support design by reducing the conductive losses between 5 and 40 mW.

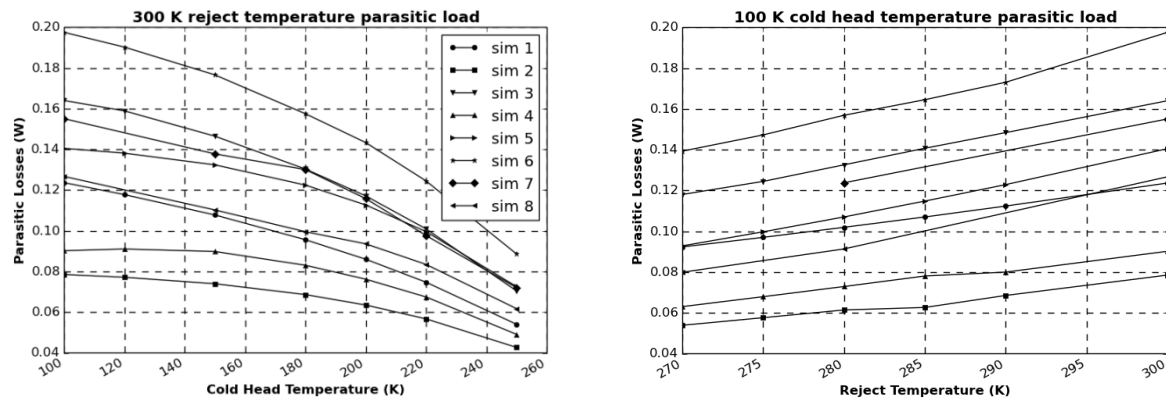


**FIGURE 4.** Shown above are the results of the simulations, for which table 1 details the different geometries utilized.

## 5. Conclusions

Our study focused on eight temperature-dependent designs for an optical refrigerator. There are several conclusions that we can draw from the systems examined here:

1. The cat's cradle design was the optimal support structure to reduce conductive losses. Aerogel's performance is not significantly worse to rule it out especially when other parameters are considered (Kevlar alignment, rigidity of system) and should still be investigated and optimized further.
2. Of the designs simulated, the "L" link supported with a Kevlar cat's cradle system in a tight enclosure best minimized the radiative and conductive losses. However, as the calculated lower bound on radiative heat transfer is approached the "Tetris" link becomes more optimal, outperforming the "L" link by a couple milliwatts. It may be possible to optimize a link that has a tortuous path to reduce absorbed fluorescence and minimize radiative losses that outperforms the proposed "L" link and "Tetris" link, but that will be left for future studies. The "L" link in a cubic enclosure is currently more desirable in that it reduces the refrigerator complexity and relaxes further requirements on enclosure size to best minimize radiative heat transfer.
3. Achieving record breaking (no load) temperatures of 93 K [5] required the reduction of the reject temperature from 300 K to 271 K. In our simulated models we predict that this could decrease the parasitic heat load anywhere from 25 – 60 mW, depending on cooler design. With the relatively small predicted efficiencies and heat lifts, proper enclosure design and heat sinking is necessary for effective OR development.
4. A prototype design with a simple "L" link with Kevlar support and larger, properly heat sunk enclosure could be built with relatively low losses and should be the first step towards a fully functioning all solid-state optical refrigerator. A more complicated enclosure around an "L" link geometry with Kevlar support would be a logical second iteration which could further reduce the combined conductive and radiative losses.

## References

- [1] Melgaard, S D, Seletskiy, D V, Di Lieto, A , Tonelli M , and Sheik-Bahae, M, Optical refrigeration to 119K, below National Institute of Standards and Technology cryogenic temperatures. *Optics Letters* **38** (9), pp. 1588-1590
- [2] Pringsheim, P. (1929). Zwei bemerkungen über den unterschied von lumineszenz und temperature-strahlung. *Z. Phys.* **57**, pp. 739-746

- [3] Melgaard, Seth D, Cryogenic optical refrigeration: Laser cooling of solids below 123K, PhD Dissertation
- [4] Seletskiy, D V , Hehlen M P , Epstein R I and Sheik-Bahae, M , Cryogenic Optical Refrigeration, *Advances in Optics and Photonics* **4** (1), 78-107
- [5] Melgaard, S D, Albrect, A, Hehlan M P ,Seletskiy, DV, and Sheik-Bahae, M, (2014) Optical refrigeration cools below 100 K. *IEEE Lasers and Electro-Optics CLEO*
- [6] Imangholi, B, Hasselbeck, P, Bender, D A, Wang, C, Sheik-Bahae, M, Epstein, R I, and Kurtz, S, (2006). Differential luminescence thermometry in semiconductor laser cooling. *Proc SPIE 6115*, pp 215-220 (2006)
- [7] Optical Refrigeration Patent Pending application number 14476351
- [8] Fletcher, Leroy S (1972). A Review of Thermal Control Materials for Metallic Junctions, *Journal of Spacecraft and Rockets* **9** pp. 849-850
- [9] Voellmer, G M, Jackson, M L, Shirron, P J, and Tuttle, J G (2003). A Cryogenic, Insulating Suspensions System for the High resolution Airborne Wideband Camera (HAWC) and submillimeter and far Infrared Experiment (SAFIRE) Adiabatic Demagnetization Refrigerators (ADRs). *Proc SPIE 4850, IR Space Telescopes and Instruments*
- [10] Rojstaczer, S, Cohn, D and Marom, G, (1985). Thermal expansion of Kevlar fibres and composites, *Journal of Materials Science Letters* **10** pp. 1233-1236
- [11] Airloy Ultramaterials (series X100) US patent no. 7,771,609 and no. 8,277,676 and application number 20120152846
- [12] Incropera, F P and Witt, D P, (1990). Introduction to Heat Transfer, John Wiley & Sons, New York, pp. 748-789
- [13] Hamilton, D C and Morgan, W R, (1952). Radiant-interchange configuration factors, *NASA TN 2836*
- [14] Acktar Nano-Black solar selective coating. <http://www.acktar.com/>
- [15] AutoCAD<sup>TM</sup>. (2013). Thermal Desktop (Version 2013)
- [16] F-Chart Software<sup>TM</sup>. (2012). EES<sup>TM</sup>. (Version 8.6)
- [17] Harris, J P, Yates, B, Batchelor, J, and Garrington, P J, (1982). The thermal conductivity of Kevlar fiber-reinforced composites. *Journal of Material Science* **17** pp. 2925-2930.
- [18] Aggarwal, R L, Ripin, D J, Ochoa, J R, and Fan, T Y, (2005). Measurement of thermo-optic properties of  $\text{Y}_3\text{Al}_5\text{O}_{12}$ ,  $\text{Lu}_3\text{Al}_5\text{O}_{12}$ ,  $\text{YAlO}_3$ ,  $\text{LiYF}_4$ ,  $\text{LiLuF}_4$ ,  $\text{BaY}_2\text{F}_8$ ,  $\text{KGd}(\text{WO}_4)_2$ , and  $\text{KY}(\text{WO}_4)_2$  laser crystals in the 80-300K temperature range. *Journal of Applied Physics* **98**
- [19] Martin K W, Schomacker, J, Fraser, T, Dodson, C, (2015). Thermal Modeling for an Optical Refrigerator. *Optical Refrigeration of Solids SPIE Photonics West*